In Vitro Assays for Nanoparticle—Cancer Cell Interaction Studies

Tomás Bauleth-Ramos and Bruno Sarmento

Abstract

Nanotechnology is a rapid-growing field with an extreme potential to revolutionize cancer treatments. However, despite the rapid advances, the clinical translation is still scarce. One of the main hurdles contributing for this setback is the lack of reliable in vitro models for preclinical testing capable of predicting the outcomes in an in vivo setting. In fact, the use of 2D monolayers, considered the gold-standard in vitro technique, leads to the creation of misleading data that might not be completely observed in in vivo or clinical setting. Thus, there is the need to use more complex models capable of better mimicking the tumor microenvironment. For that purpose, the development and use of multicellular tumor spheroids, three-dimensional (3D) cell cultures which recapitulate numerous aspects of the tumors, represents an advantageous approach to test the developed anticancer therapies. In this chapter, we identify and discuss the advantages of the use of these 3D cellular models compared to the 2D models and how they can be utilized to study nanoparticle-cancer cell interaction in a more reliable way to predict the treatment outcome in vivo.

Keywords

Nanoparticles · Spheroids · Cancer · Tumor microenvironment · 3D · In Vitro · Nanotechnology · Extracellular matrix · Distribution · Efficacy · Toxicity · High throughput screening

1 Introduction

Cancer, a complex and multifactorial disease, is one of the major threats to global health due to its high rates of incidence and mortality. In fact, this disease is one of the leading causes of death worldwide having, according to the report on global burden of cancer worldwide (GLOBOCAN 2018) by the World Health Organization (WHO), been responsible for 9.6 million deaths in 2018. Moreover, it is expected that this value will keep increasing over the years [1].

Commonly, anticancer therapy relies, on the initial stage, on chemotherapy treatment in order to reduce the tumor mass followed, if possible, by surgery to remove the rest of the tumor. Subsequently, chemotherapy and radiotherapy are applied to eliminate the remaining cancer cells [2]. Despite being the main strategy, this method still faces many hurdles as the existence of numerous and severe adverse effects, due to the nonspecificity of these approaches. Furthermore, chemotherapeutics also show lack of efficacy due to their physicochemical characteristics, leading to poor accumulation in the tumor site, short blood circulation, and the existence of tumor resistance mechanisms [3].

Nanoparticles (NPs), owing to their physicochemical properties, have emerged as powerful tools to improve cancer

T. Bauleth-Ramos
i3S – Instituto de Investigação e Inovação em Saúde, University of Porto, Porto, Portugal

INEB – Instituto de Engenharia Biomédica, University of Porto, Porto, Portugal

ICBAS, Instituto Ciências Biomédicas Abel Salazar, University of Porto, Porto, Portugal

Drug Research Program, Division of Pharmaceutical Chemistry and Technology, Faculty of Pharmacy, University of Helsinki, Helsinki, Finland

B. Sarmento (✉)
i3S – Instituto de Investigação e Inovação em Saúde, University of Porto, Porto, Portugal

INEB – Instituto de Engenharia Biomédica, University of Porto, Porto, Portugal

CESPU, Instituto de Investigação e Formação Avançada em Ciências e Tecnologias da Saúde & Instituto Universitário de Ciências da Saúde, Gandra, Portugal
e-mail: bruno.sarmento@ineb.up.pt

F. Fontana, H. A. Santos (eds.), *Bio-Nanomedicine for Cancer Therapy*, Advances in Experimental Medicine and Biology 1295, https://doi.org/10.1007/978-3-030-58174-9_10

treatments and counteract the aforementioned hurdles [4–6]. Nowadays, it is possible to produce NPs from a myriad of materials (polymers, lipids, inorganic materials, etc.) and precisely tune their production to achieve specific characteristics [4, 7]. Hence, NPs can be produced to load different types of molecules, control their pharmacokinetic and pharmacodynamic profiles, protect them from degradation, and increase their stability and accumulation in the targeted tissues [8]. Altogether, it permits to boost the therapeutic effect of the treatments while diminishing their off-target side effects.

However, while NPs have been showing promising results in preclinical testing, their clinical translation is still limited [4]. One of the major hurdles for NP clinical translation is the lack of preclinical models that can resemble the heterogeneity of the different tumors and their phenotypes [9–11]. In fact, NP interaction with cancer cells is usually tested in in vitro 2D cellular models which lack the complexity of biological tissues and thereby cannot fully replicate the existence of diverse physiological barriers and the interplay between the different components of the tumors (e.g., cells, extracellular matrix, soluble molecules). Thus, these assays can only provide limited results which ultimately do not correspond to what is observed on an in vivo and clinical setting. It is then imperative to develop new relevant in vitro cancer models capable of better recapitulating the tumor microenvironment (TME) [11].

The development of three-dimensional (3D) cellular models, which mimic several aspects of the TME, can bridge the gap between 2D models and in vivo and ease the development and screening of new nanomedicines for cancer treatment [9, 12]. By using these more accurate models, it is possible to obtain more reliable results and also use them to tune the NP properties based on the biology of the target population, leading to the development of effective therapies [9].

Hence, in this chapter we present an overview on 3D in vitro models to study the interaction between NPs and cancer cells in order to better predict the outcome of the treatments and facilitate the translation of the therapies.

2 2D Versus 3D Models

To date, two-dimensional (2D) cell culture monolayer models have been the gold-standard technique to preclinically develop and study anticancer therapies, due to their easiness, simplicity, reproducibility, quickness, and low cost [13–15]. These models are mostly produced from immortal tumor cell lines, as they are an unlimited self-replicating source capable of growing in large quantities [16]. Additionally, these cell lines are relatively molecular homogeneous, and their genetic profile is known and described [16]. To increase the predictive value of the gathered data, it is possible to use primary cells isolated from living tissue [17, 18]. Although these cells maintain the genomic and phenotypic profiles of the descendant tissue, they are hard to culture and have limited self-replication, which hamper their use [18]. Moreover, 2D models cannot mimic crucial aspects from the tumors, such as the heterogenicity of the TME, composed by various types of cells and noncellular structures as the extracellular matrix (ECM), failing to emulate the in vivo conditions and provide physiological relevance. The existent 3D spatial conformation of tumors results in a heterogeneous and diffusion-limited exposure to various nutrients, signaling molecules, oxygen, and metabolites, among other physical and chemical cues, which cannot be mirrored in 2D cultures [19–22]. Moreover, this 3D spatial organization is also known to influence cell-cell interactions, impacting their morphology, adhesion, viability, proliferation, and biological response to soluble factors and physical stimuli [23–25]. For example, these morphological and biological changes are responsible for a slower proliferation rate of cells in 3D compared to 2D models [26, 27], impacting their response to different compounds, including anticancer molecules [27]. As such, 2D models, by failing to simulate the reciprocal interactions between different cells and the TME, influence the obtained outcomes to the tested therapies, leading in the end to poor prediction of their real in vivo effect.

To avoid the production of misleading preclinical data and improve the translation of new anticancer therapies, there is the need to bridge the gap between 2D models, in vivo whole-animal tumor models, and clinical trials. To that end, 3D cellular models have been extensively studied as they permit the simulation of numerous physiological aspects of the tumors, being more relevant and better predictive models than the 2D ones [12, 20, 28, 29]. In the past decades, various 3D models have been developed, including microfluidic models, scaffold-based models, tumor tissue explant models, and multicellular tumor spheroids (MCTS) [30].

2.1 Multicellular Tumor Spheroid Production Techniques

MCTS are formed without resorting to any exogenous artificial platforms to promote cell growth [31]. To produce MCTS, several techniques can be applied, being the most commonly used agitation-based, hanging drop, and liquid overlay techniques (Fig. 1). All these techniques have as base the use of nonadherent surfaces to promote cell-cell interactions and consequent aggregation [31]. In agitation-based techniques, single-cell suspensions are kept agitating, for example, in spinner flasks, in order to reduce the effect of gravity and promote spontaneous aggregation [32, 33]. While this method is appropriate for long-term culture and

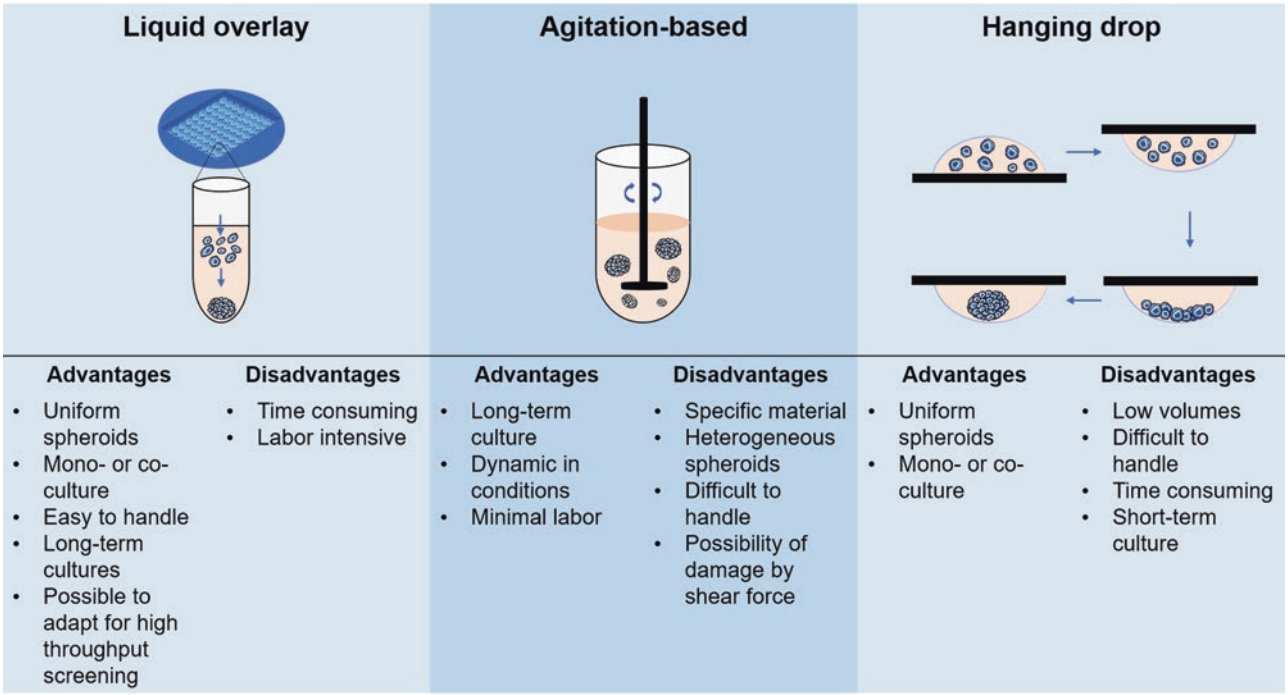

Fig. 1 Multicellular tumor spheroid production techniques, their advantages, and limitations. (Imaged partly generated using Servier Medical Art)

can mimic the dynamic conditions found in the body, it carries several disadvantages as the need of specific material, formation of heterogeneous spheroids, and difficulty to handle [34]. Moreover, the shear fluid force may induce damage and/or changes in the used cells [35]. In the hanging drop method, cell cultures are suspended and due to the gravitational forces cells tend to sediment and spontaneously aggregate in the liquid-air interface [36]. Using this method it is possible to produce uniform spheroids of mono- and co-cultures [37]. However, since spheroids are suspended in a low volume of media, it is time-consuming and difficult to handle and cannot be maintained for long periods [37]. At last, liquid overlay technique represents a more convenient and easier procedure, capable of producing uniform spheroids and which is possible to adapt for high-throughput screening (HTS) [33]. In this technique, cell suspensions are placed in nonadherent surfaces, as agarose or poly(2-hydroxyethyl methacrylate) (poly-HEMA), enhancing cell-cell interactions in spite of the cell-surface interactions [38]. Currently, it is possible to use commercial molds in which these materials (e.g., agarose) are casted, allowing the simultaneous production of numerous spheroids in a homogeneous manner [39, 40].

2.2 MCTS Advantages

MCTS are one of the most commonly used 3D tumor models, consisting of spherical cellular self-aggregates that produce their own ECM, being capable of recapitulating several aspects of the TME, and are recognized as nonvascularized tumor models [41]. This type of model possesses a similar growth kinetics to real tumors, starting with an exponential cell expansion, followed by a delayed growth due to a decrease in proliferative cells, and increase in quiescent and necrotic cells [42]. As the MCTS grow, a gradient of oxygen, nutrients, and metabolic waste is formed, leading to an hypoxic core with necrotic cells and an outer rim formed by proliferative cells in the outer layer and quiescent cells in the inner layer. This hollow structure is estimated to be formed in spheroids with diameter over 400–500 μm, with the outer rim having usually 100–220 μm of thickness [42–45]. Furthermore, combined with the formed 3D spatial organization and its cell-cell and cell-ECM interactions, this leads to cellular heterogeneity, affecting protein expression and leading to different genetic profiles, which were found to resemble the physiological conditions existent in human tumors [46]. These protein expression and genetic changes highly impact the function of different anticancer therapies, inducing several mechanisms of drug resistance [47]. Another aspect of human tumors that is recapitulated in MCTS is the existence of an acidic microenvironment. Due to the generation of a hypoxic core, tumor cells, in response to the lack of oxygen, increase the production of lactate, which promotes an acidification of the microenvironment (pH 6.5–7.2) [28, 48]. This acidic TME directly impacts anticancer molecules protonation, influencing their uptake and efficacy [49].

Additionally, MCTS can be optimized to mimic the cellular heterogeneity of human tumors by co-culturing tumor cells with different stromal cells as fibroblasts, as well as immune and endothelial cells [50, 51]. It is known that the intricate relationship of tumor and stromal cells promotes several pro-tumor events as angiogenesis, invasion, metastasis, and resistance to anticancer drugs [51, 52]. Stromal cells will influence tumor cell activity by secreting soluble factors (e.g., cytokines and growth factors) [53], producing ECM proteins, which interact with different signaling pathways [54] and that create a physical barrier that limits the penetration of different molecules [55, 56]. Altogether, these factors contribute to a higher resistance of the tumor cells to the anticancer treatments when compared with 2D models, resembling in a better fashion what happens in an in vivo situation (Fig. 2).

Also, the ability to produce uniform spheroids with mono- and co-cultures; to tailor their size and controlling their properties, for example, by adjusting the initial cell density and duration of culture; and to use them for HTS purposes makes them valuable tools to study tumor biology and treatment. For instance, spheroids can be used to study the signaling cross talk in the TME, tumor cell growth kinetics, migration and invasion, and the response to several anticancer therapies, including radiotherapy, chemotherapy, immunotherapy, and the use of biomaterials such as nanoparticles [15, 57, 58].

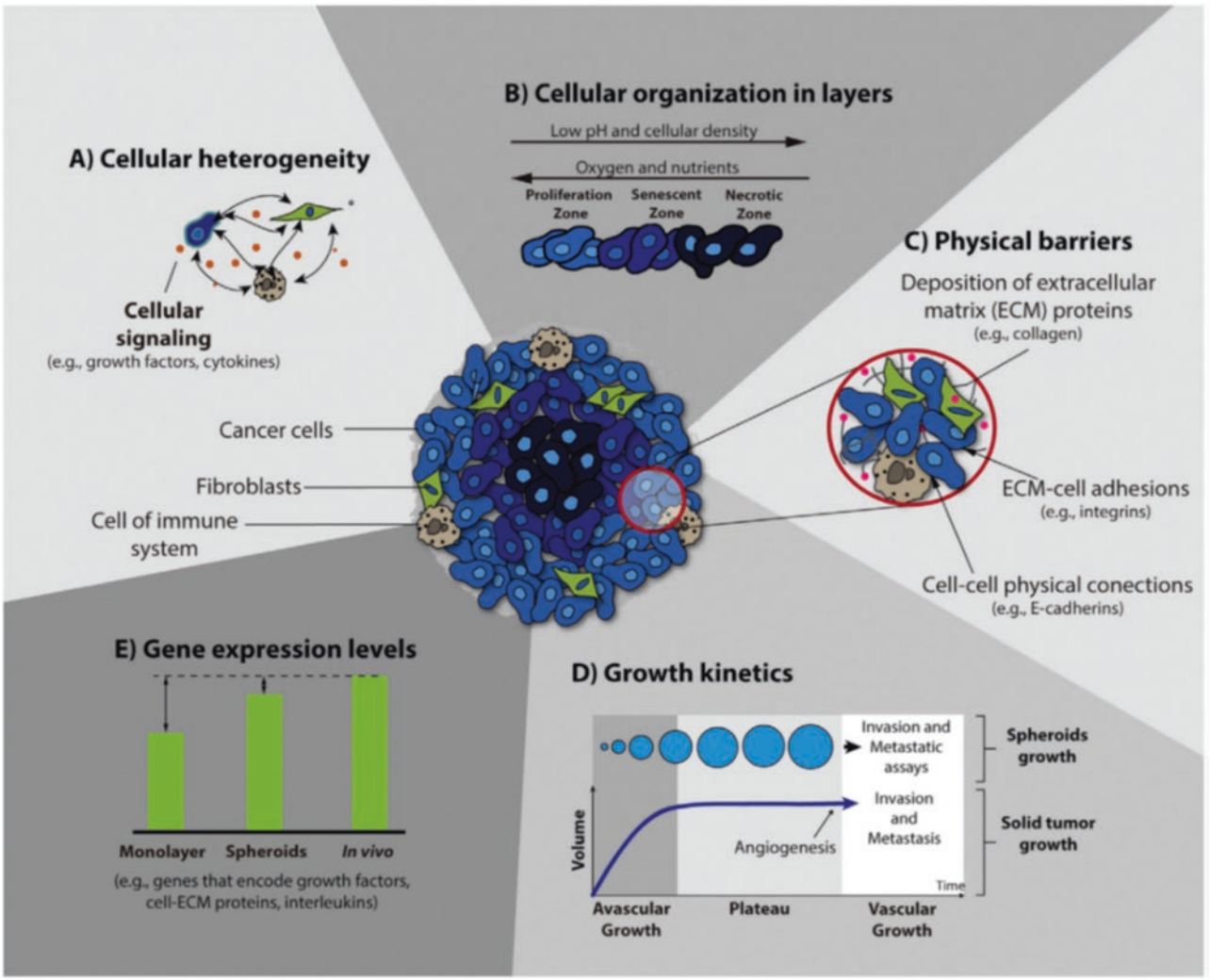

Fig. 2 Main aspects of 3D spheroids that recapitulate tumor characteristics and are essential for anticancer therapy screening. (**a**) Heterogenicity of tumors (cancer and stromal cells). (**b**) Gradient of nutrients, oxygen, and pH, formation of necrotic core, and senescent and proliferative layers. (**c**) Formation of physical barrier by extracellular matrix deposition and cell-cell interaction. (**d**) Correlation between the growth kinetics of spheroids and solid tumors: initial exponential growth (avascular growth phase) and plateau state. (**e**) Closer gene expression patterns to in vivo solid tumors. (Reprinted with permission from Ref. [55])

2.3 Disadvantages/Limitations

Despite the current advances, the employment of 3D models for preclinical testing still faces several adversities. The major existent shortcomings are the lack of standardization in terms of protocols for spheroid production and evaluation/testing (e.g., characterization, imaging, drug and other therapies screening purposes), high costs, highly laborious, cell-type limitation to form spheroids, and difficulty to produce homogeneous spheroids for HTS purposes [59, 60]. However, the use of 3D models for preclinical testing is growing exponentially [61], and in the next years, with the advances on 3D model formation and standardization of the characterization and testing assays, they will likely substitute 2D cell culture models for in vitro preclinical research [62].

3 Multicellular Tumor Spheroids for Assessing Nanomaterials

One important application of MCTS is to test the cellular association, biocompatibility, and efficacy of nanomaterials, as it can provide valuable data on their interaction and effect in the tumors, as well as in the specifically in the different components of the TME, predicting their impact in vivo. Therefore, it allows to improve the nanoformulations before proceeding to animal studies, reducing the number of used animals and expediting the development of successful therapies. Thus, it is of utmost importance to start testing the developed nanomaterials in more relevant models than the standard 2D cultures, since 2D models can create misleading data.

3.1 Cellular Association/Tumor Penetration

When assessing NP cellular association, the absence of ECM which creates a physical barrier and diffusion gradient through tissue highly impacts the results in 2D when compared to 3D [63, 64]. For instance, even if high cellular uptake is observed both in the 2D and 3D cell models, in the 3D cell model, the NPs might be predominately taken up by cells in the periphery without being able to deeply penetrate in the tumor [42]. This will consequently have an effect on the antiproliferative ability of the developed nanosystems, which might show a higher effect on the 2D cell models (i.e., a lower IC_{50} value) [65, 66]. Furthermore, several studies have shown a correlation between high NPs and drug accumulation and penetration, with an enhanced cytotoxic effect [67, 68]. Thus, the use of MCTS is extremely useful to study the penetration ability of the NPs into the tumors and assess their anticancer efficacy [33].

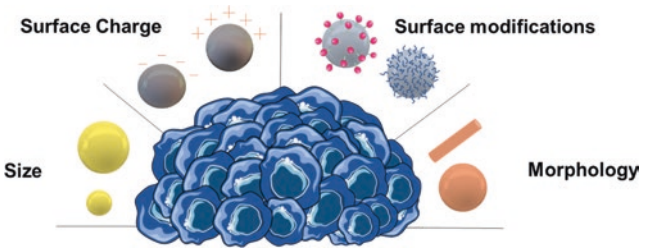

Fig. 3 Illustration of the physicochemical characteristics that affect NP interaction with the tumors. (Imaged partly generated using Servier Medical Art)

It is known that the physicochemical characteristics (e.g., size, charge, morphology, and surface functionalization) of the NPs will highly impact their interaction and penetration into tumors (Fig. 3). Therefore, this subsection will discuss the impact of the NP physicochemical properties on interaction cells in 3D in vitro models and compare to 2D in vitro cellular models and in vivo assays (Table 1).

3.1.1 Size

The size of the NPs is one of the most crucial parameters affecting their interaction with cancer cells. Thus, several studies have been performed to try to analyze its impact in the penetration and uptake of NPs in tumors. For example, in one study, Tchoryk et al. [69] have cultured HCT116 colorectal cancer spheroids and incubated them with polystyrene NPs with different sizes (30, 50, and 100 nm) (Fig. 4). After 24 h incubation, the smaller NPs (30 and 50 nm) were taken up by over 90% of the cells, while the larger particles (100 nm) were only taken up by 22%. Furthermore, while the smaller NPs were able to reach the core of the spheroid, the larger NPs were mainly located in the periphery. This study demonstrated a size-dependent uptake and penetration of NPs into tumors. Another study [70], also using polystyrene NPs but with bigger sizes (20, 100, and 500 nm), has compared in vitro cellular uptake and penetration in 2D monolayers of pancreatic cancer cells (BxPC-3 and PANC-1) and in spheroids prepared with the same cell lines. Interestingly, in this study it was found that there was a size-dependent uptake in BxPC-3 monolayers ($20 > 100 > 500$ nm), while in PANC-1 monolayers, 100 nm NPs were the ones with higher uptake. This was attributed to the fact that BxPC-3 cells exclusively used clathrin-dependent mechanisms for the uptake of all the NPs and in PANC-1 cells, there were multiple endocytic routes involved in the uptake of 100 nm NPs and only one mechanism for NPs with the other sizes. Further, when incubated with the spheroids, it was observed a size-dependent uptake, showing linear correlation with the BxPC-3 cellular uptake in 2D and no correlation with the data obtained with the PANC-1. This has shown that the mechanisms of uptake, transport, and penetration may vary between the 2D and 3D in vitro models

Table 1 Overview of the main physicochemical characteristics influencing the interaction of NPs with tumor cells. 2D, 3D, and in vivo assays

Size (nm)	Type of NPs	2D model		3D model			In vivo			References
		Cells	Outcome	Cells and cell density at day 0	Technique of production	Outcome	Animal model/cell lines	Route of injection	Outcome	
2 6 15	Gold NPs (spherical, negatively charged)	MCF-7	No observed toxicity Size-dependent uptake: 2 ≫ 6 = 15 NP location: 2 and 6 nm – cytoplasm and nucleus 15 nm – cytoplasm	MCF-7 600 cells/well	Liquid overlay technique	Size-dependent uptake: 2 > 6 > 15 Time dependency was only observed for NPs with size 2 and 6 nm These NPs were also able to penetrate deeper into the spheroid and localize both in the outer and inner layers 15 nm NPs showed lower penetration and were localized mostly on the outer layers	Balb/c nude mice with MCF-7 cells	IV 5 mg Au/Kg	Rapid elimination from blood in time and size-dependent manner: 15 > 6 > 2 Size-dependent tumor accumulation: 2 > 6 > 15	[72]
50 100			No observed toxicity Size-dependent uptake: 50 > 100 (5-fold higher uptake) Localized on the cytoplasm			Mostly located on the periphery Size-dependent penetration 50 > 100 (fourfold higher) Time-dependent penetration only for 50 nm NPs			Rapid elimination from blood in time- and size-dependent manner: 100 > 50 Size-dependent tumor accumulation: 50 > 100	[71]
30	Polystyrene NPs (negatively charged)	–	–	HCT116 2000 cells/well	Liquid overlay technique	30 nm: 70% uptake after 2 h and >90% after 6 h incubation Have shown the highest penetration ability	–	–	–	[69]
50						50 nm: 80% uptake after 2 h and >90% after 6 h incubation				

100						100 nm: < 10% uptake after 2 h and 22% after 24 h incubation Most of NPs in the periphery, low penetration				
20	Polystyrene NPs (spherical, negatively charged)	BxPC-3 and PANC-1 and NIH3T3	10-fold and 50-fold higher cellular uptake in BxPC-3 than 100 and 500 nm NPs, respectively owest uptake by PANC-1 Only one mechanism of uptake is utilized by PANC-1 cells for internalization	BxPC-3 500 cells/well and PANC-1 120 cells/well and PANC-1/ NIH3T3 (120:12)	Liquid overlay technique	BxPC3 spheroid: 20 nm NPs penetrate more effectively than bigger NPs There was no penetration and almost absent cellular uptake by cells in the periphery of 500 nm NPs Linear correlation with cellular uptake in 2D	–	–	–	[70]
100			Higher cellular uptake in PANC-1 cells than the other NPs Several mechanisms of uptake are utilized by PANC-1 cells for internalization	cells/well		PANC-1 spheroids: 20 nm NPs had higher penetration and reached the core. 100 nm NPs could also penetrate but reached the core in less extent				

(continued)

Table 1 (continued)

Size (nm)	Type of NPs	2D model		3D model			In vivo			References
		Cells	Outcome	Cells and cell density at day 0	Technique of production	Outcome	Animal model/cell lines	Route of injection	Outcome	
500			Internalization in BxPC-3 cells was almost absent Only one mechanism of uptake is utilized by PANC-1 cells for internalization			500 nm NPs could only penetrate the surface layers No correlation with 2D data PANC-1/ NIH3T3 spheroids: Less permeable model. NPs could not reach the core. 500 nm NPs only accumulated in the periphery 100 nm NPs accumulated more efficiently than 20 nm NPs due to transcytosis mediated by the fibroblasts				
30	Silica NPs (negatively charged)	–	–	4T1 and 3T3 and 3T3/4T1 (1:1 and 5:1) 18,500 cells/ well	Liquid overlay technique	30 nm NPs had higher penetration in all the spheroids In spheroids without fibroblasts, both NPs were able to penetrate (70–80% positive area) Increased in number of fibroblasts inhibited NP penetration	–	–	–	[106]
100		–	–							

Surface charge (mV)	Type of NPs	2D model		3D model			In vivo			References
		Cells and cell density at day 0	Outcome	Cells and cell density at day 0	Technique of production	Outcome	Animal model/cell lines	Route of injection	Outcome	
53 ± 7	DOTAP liposomes	–	–	Lewis lung carcinoma (LLC) cells. 1000 cells/well	Liquid overlay technique	High-cell bind and higher accumulation in the spheroid. Consequent enhanced cytotoxic effect when loaded with paclitaxel	–	–	–	[67]

−56 ± 3	DOPS liposome			cells/well		Low cell binding but higher penetration into the spheroids than the DOTAP liposomes (cationic NPs)				
24 ± 2	Polystyrene NPs (50 nm)-NH_2	–	–	HCT116 colon cancer cells. 2000 cells/well	Liquid overlay technique	Poor penetration Mostly located in the periphery of the spheroid	–	–	–	[69]
−32 ± 3	Polystyrene NPs (50 nm)-COOH			2000 cells/well		Poor penetration and no accumulation on the periphery				
−32	Plain polystyrene NPs (50 nm)					Fast and high penetration homogeneous distribution within the spheroid				
−20 −40	Silica NPs	–	–	4T1 and 3T3 and 3T3/4T1 (1:1 and 5:1) 18,500 cells/ well	Liquid overlay technique	Less negative NPs penetrated less deeply Penetration was inversely correlated to the number of fibroblasts	–	–	–	[106]
21.5–23.5 −22.2 −9 −8	Modified PEG-b-PLA NPs	–	–	MDA-MB-231	Liquid overlay technique	Rapid accumulation of positive NPs in the periphery Negatively charged NPs showed low penetration	Balb/c nude mice with MDA-MB-231 cells	IV	Positive NPs were able to extravasate and accumulate in the tumors, contrary to the other NPs	[107]
Shape	**Type of NPs**	**2D model**		**3D model**			**In vivo**			**References**
		Cells and cell density at day 0	**Outcome**	**Cells and cell density at day 0**	**Technique of production**	**Outcome**	**Animal model/cell lines**	**Route of injection**	**Outcome**	
Spherical Rods	Gold-silica core-shell NPs (negatively charged)	HeLa	Rods were taken up at a higher extension than spheres, leading to higher drug accumulation	HeLa 12,345 cells/ well	Liquid overlay technique	Spheres had a more uniform distribution in the spheroids, penetrating deeply into the cell layers (able to penetrate) contrary to the rod NPs	–	–	–	[81]

(continued)

Table 1 (continued)

Size (nm)	Type of NPs	2D model		3D model			In vivo			References
		Cells	Outcome	Cells and cell density at day 0	Technique of production	Outcome	Animal model/cell lines	Route of injection	Outcome	
Spherical (AR = 1) Elongated (AR = 2.8) Elongated (AR = 7.5)	Polystyrene NPs (positively charged)	HeLa	Spherical NPs were taken up at a higher extent Cellular uptake was dependent on the AR. Higher AR, lower uptake	HeLa 800 cells/well	Liquid overlay technique	Elongated NPs with lower AR were able to penetrate and accumulate at a higher extent than the other NPs	–	–	–	[86]
Surface modifications	**Type of NPs**	**2D model**		**3D model**			**In vivo**			**References**
		Cells and cell density at day 0	**Outcome**	**Cells and cell density at day 0**	**Technique of production**	**Outcome**	**Animal model/cell lines**	**Route of injection**	**Outcome**	
iRGD DSS	Lignin NPs	PC3-MM2 MDA-MB-231 A549	Both iRGD and DSS ligands increased uptake PC3-MM2: DSS > iRGD > plain MDA-MB-231: DSS > iRGD = plain A549: DSS > plain > iRGD	PC3-MM2 5000 cells/well MDA-MB-231 7000 cells/well A549 7000 cells/well	3D bioprinting (magnets)	Both iRGD and DSS ligands increased uptake PC3-MM2: DSS > iRGD > plain MDA-MB-231: DSS = iRGD > plain A549: DSS > iRGD = plain When loaded with a chemotherapeutic, the IC_{50} values were higher than in 2D culture. Moreover, only in the PC3-MM2 cells, the IC_{50} values for modified NPs were lower than for plain NPs	–	–	–	[88]
Anti-FGFR3	Silica NPs			RT4 150,000 cells/well	Liquid overlay technique	Fourfold enhanced internalization of NPs modified with the anti-FGFR3 antibody compared to unmodified NPs NPs modified with antibody partially inhibited cell proliferation and spheroid growth	–	–	–	[90]

tLyP-1	Micelles	4T1	Fourfold enhanced cellular uptake after NP modification	4T1 10,000 cells/well	Liquid overlay technique	The peptide enhanced the uptake by the spheroids but led to lower penetration than unmodified NPs	4T1	IT IV	IT: NPs modified with the peptide showed stronger penetration ability	[89]
									IV: Peptide-modified NPs had target effect and higher accumulation overtime. Further, these NPs were able to deeply penetrate into the tumors	
Anti-TfR	Lipid magnetic nanovectors	–	–	U-87 MG 25,000 cells/drop	Hanging drop	NPs modified with antibody had a remarkable enhanced uptake after 48 h compared to unmodified NPs (40% compared to 8%)	–	–	–	[93]
						Enhanced uptake led to enhanced antiproliferative effect after stimulation:				
						Antibody-modified NPs: 49.6% healthy cells, 38.8% necrotic cells, 4.9% apoptotic cells, and 6.7% of late apoptotic cells				
						Unmodified NPs: >96% of healthy cells				

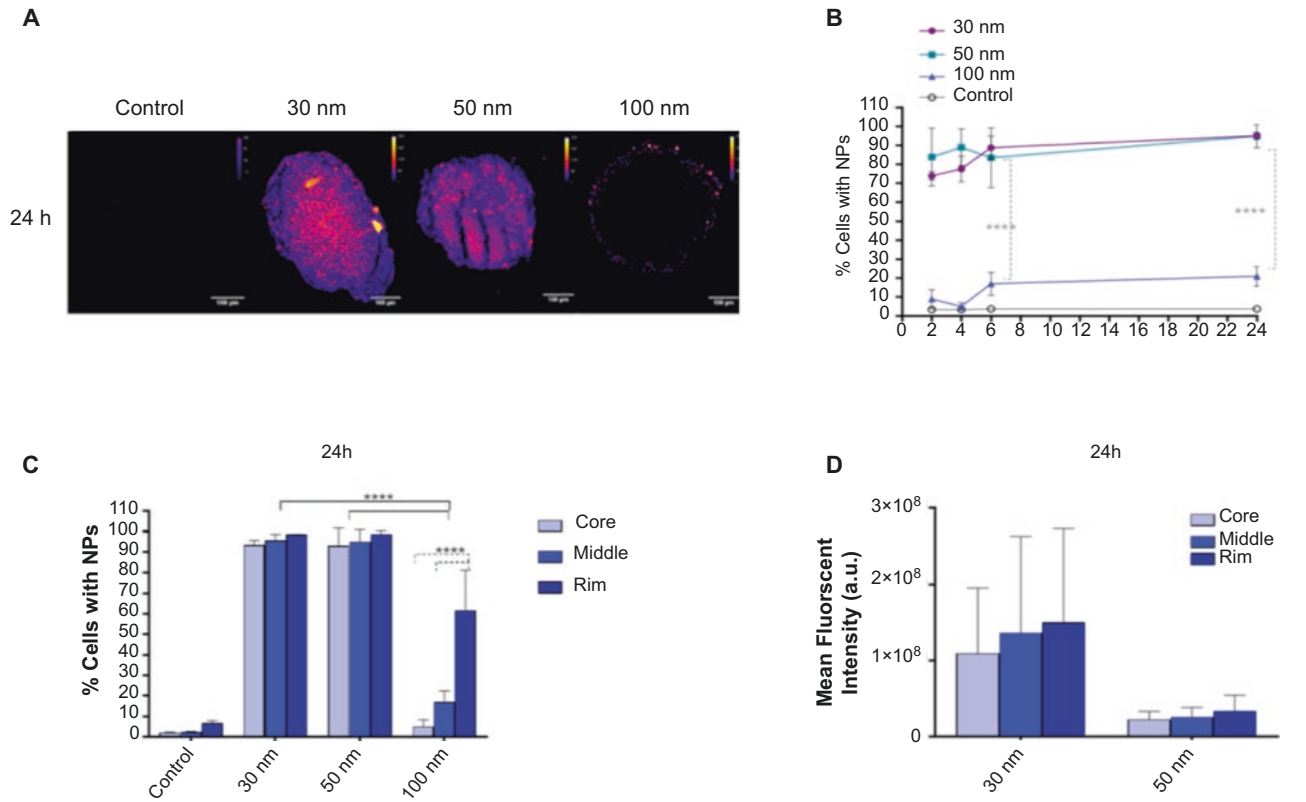

Fig. 4 Size-dependent penetration of polystyrene NPs with sizes of 30, 50, 100 nm after 24 h incubation with HCT116 spheroids. (**a**) Confocal microscopy images of HCT116 spheroid cross-sections after incubation with the NPs. (**b**) Overtime NP penetration into spheroids measured by flow cytometry. (**c**, **d**) Distribution of the NPs in the spheroids. (Adapted with permission from Ref. [69])

and between different 3D models. Like the previously mentioned study, only the smaller NPs could penetrate into the tumors, while the others were mainly retained in the periphery of the spheroid. Moreover, the addition of fibroblasts to the spheroid model significantly enhanced ECM deposition, leading to a poorer penetration of the NPs into the spheroid and blocking their access to the core. However, due to transcytosis mediated by fibroblasts, 100 nm NPs accumulated more efficiently than the other NPs.

Other studies using gold NPs with size ranging from 2 to 100 nm (2, 6, 15, 50, and 100 nm) [71, 72] have also shown a size-dependent uptake and penetration of the NPs in 2D monolayers and spheroids, with the smaller NPs being taken up and penetrating in a higher extent. NPs with size >15 nm were found mainly in the periphery of the spheroids, showing similar pattern to what was observed in the aforementioned studies. Moreover, in these studies, there was correlation between the in vitro results and the in vivo, where it was also observed a size-dependent tumor accumulation after intravenous injection of the NPs.

Taking this into account, it is possible to observe that smaller NPs (<100 nm) have a higher penetration in spheroids [67, 71–73], while larger NPs, despite having limited penetration, may accumulate in spheroids' periphery. Moreover, several studies have found that 50 nm is the optimal size for a better balance between NP penetration and accumulation [71, 74].

3.1.2 Surface Charge

Surface charge is another critical parameter with high influence in NP penetration and accumulation in tumors, and that can be studied using 3D in vitro cellular models [68, 75]. For example, Solomon et al. [67] incubated lung cancer spheroids with positively (53 ± 7 mV) and negatively (−56 ± 3 mV) charged liposomes for 1 h and analyzed their uptake and ability to penetrate in the tumor spheroids. Positively charged NPs were taken up at a higher extent than negatively charged NPs, possibly due to interaction of the NPs with the negatively charged membranes of the cells. Moreover, positively charged NPs accumulated in the periphery of the spheroid, with low capacity of penetration, while the negatively charged NPs were able to penetrate the spheroid. Interestingly, after loading these NPs with a chemotherapeutic drug (paclitaxel), it was observed a higher cytotoxic effect for the positive NPs, attributed to a higher accumulation of the NPs and consequently of the drug, even if in the periphery of the spheroid. Similar findings were obtained in other studies, for example, using positively and negatively charged liposomes

in melanoma spheroids [76] and positively and negatively charged gold NPs in breast cancer spheroids [77], with positive NPs accumulating in the periphery and negative NPs being able to penetrate into the core of the spheroids. Moreover, negative gold NPs contrarily to positive NPs were able to induce a higher hyperthermia effect after being radiated by near-infrared laser [77].

The same observations were not totally obtained in a different study performed by Tchoryk et al. [69] In this study, 50 nm polystyrene NPs positively charged (aminated) and negatively charged (carboxylated or plain NPs) were incubated for 24 h with HCT116 colorectal cancer spheroids. As expected, positively charged aminated NPs were highly taken up, and their penetration was limited to the outer cell layers of the spheroids. However, while negatively charged plain NPs were also able to be highly taken up by the cancer cells and penetrate deeply into the spheroid, negatively charged carboxylated NPs were only taken up at a low extent (20% after 24 h) and could barely penetrate the spheroid. The authors justify this due to the different protein content that might be adsorbed to the NPs upon protein corona formation. This highlights that both the surface charge and also the constitution of the NPs have an effect on NP interaction that should be considered. Also, it is hypothesized that the presence of ECM restricts the diffusion of charged NPs due to electrostatic interactions [78].

Altogether, these findings allow to rationally tailor the NPs according to the needs of the treatment, taking into consideration that positively charged NPs are commonly retained in the superficial layers of spheroids, while negatively charged NPs, depending on their surface chemistry, are able to penetrate deeper into the spheroids [67, 79]. Furthermore, while positive charge might impede NP deep penetration into the tumor tissue, it can enhance their retention [79, 80].

3.1.3 Shape

Shape is another factor impacting the NPs' interaction with tumors and whose influence can be studied using MCTS. Some studies in MCTS have shown that rod-shaped NPs have a faster diffusion rate and extended accumulation than spherical NPs [81–83], which is in agreement with in vitro and in vivo observations [84, 85]. For example, Zhang et al. [86] have produced three types of polystyrene NPs with different shapes (spherical and elongated) and aspect ratio (AR) but with fixed volume, identical chemical composition, and similar surface charge (+50 mV) (Fig. 5). The produced NPs were incubated with HeLa cells in 2D monolayer and HeLa spheroids, and their uptake and penetration was evaluated. In the 2D culture, the cellular uptake was directly related to the AR, as a decreased AR lead to higher cellular uptake, with spherical NPs being taken up more extensively than rod-shaped NPs. Contrariwise, short rod-shaped NPs had a higher uptake and penetration in spheroids than spherical NPs and long rod-shaped NPs. However, it is difficult to generate NPs with comparable parameters, for which there is still limited information in the literature and several contradictory reports [42, 83].

3.1.4 Surface Modifications

MCTS are also an important tool to comprehend and evaluate how different surface modifications, for example, to avoid clearance and prolong lifetime of the NPs or to improve treatment by targeting specific cells, etc., affect the penetration in tumors. For example, PEGylation of NPs, commonly used to prolong their blood circulation time, was shown to reduce NP accumulation in spheroids [67, 79, 80] and increase NP penetration [42, 87].

The use of targeting moieties and cell-penetrating peptides can increase the uptake of NPs by the spheroids. In order to assess the efficacy of using targeting moieties on NPs for enhanced tumor uptake and anticancer efficacy, Figueiredo et al. [88] performed an extensive study testing modified lignin NPs in three different cell lines, PC3-MM2 (prostate cancer), MDA-MB-231 (breast cancer), and A549 (lung cancer), both in 2D monolayers and 3D MCTS model (Fig. 6). Here, lignin NPs were modified with either the dentin phosphophoryn-derived (DSS) or with iRGD cell-penetrating peptides, forming spherical NPs with size ca. 300 nm and surface charge of −25 mV. Unmodified and modified NPs were incubated with the cells both in 2D and 3D, and their uptake was analyzed by confocal microscopy and flow cytometry. In both cellular models, NPs modified with DSS had an enhanced internalization in all the cells lines compared to the control, while iRGD-NPs had an enhanced internalization in PC3-MM2 and MDA-MB-231 cells but not on A549. However, in general, the cellular uptake in 2D was superior to the cellular uptake in 3D. The NPs were then loaded with a chemotherapeutic and their anticancer efficacy assessed in the same models. Interestingly, in the 2D models, despite the difference in uptake of modified NPs, there were barely any differences in the IC_{50} of the different treatments. However, in the MCTS models, modified NPs were able to induce an enhanced antiproliferative effect on the PC3-MM2 MCTS model, while no differences were observed on the other models. Nonetheless, the IC_{50} obtained in 2D were lower than the ones obtained in the 3D models, displaying a higher resistance to the treatment that might be encountered in vivo. In another study, Wang et al. [89] have modified NPs with a targeting peptide (tLyP-1), which promotes tumor homing and penetration, and studied its targeting ability in 2D monoculture, in spheroids, and in an in vivo tumor model of 4 T1 breast cancer cells. Modified NPs presented increased uptake in 2D and in the MCTS, being able to penetrate into the spheroid. Furthermore, in vivo, the targeting ligand also enhanced the penetration of NPs after intratumoral injection and enhanced the accumula-

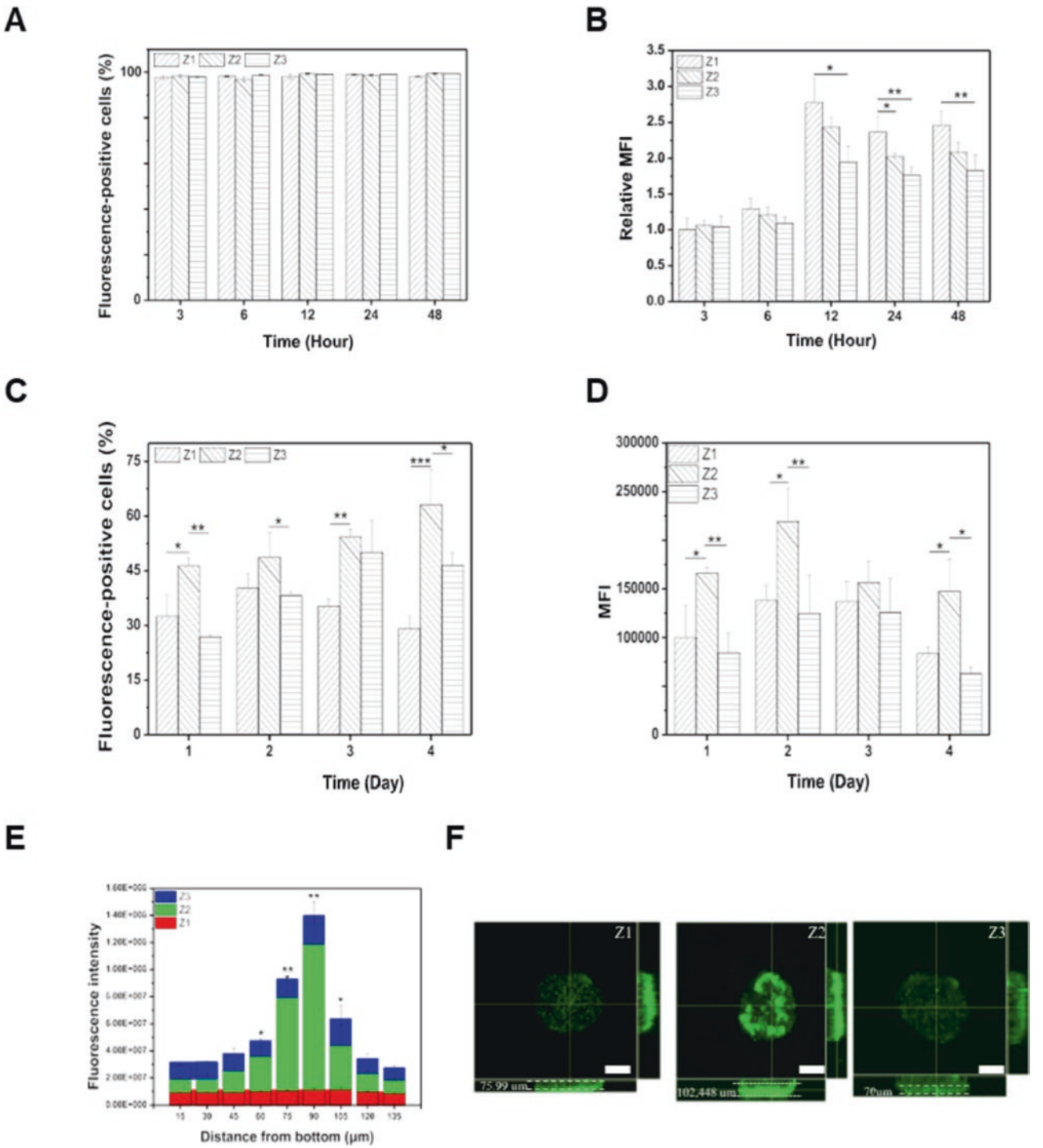

Fig. 5 (**a**) Quantitative cellular uptake of Z1 (spherical, AR = 1), Z2 (elongated, AR = 2.8), and Z3 (elongated, AR = 7.5) polystyrene NPs after incubation with HeLa cell monolayer. (**b**) And respective MFI. (**c**) Quantitative cellular uptake of Z1, Z2, and Z3 polystyrene NPs after incubation with HeLa cell spheroids. (**d**) And respective MFI. (**e**) Analysis of NP penetration in HeLa spheroids. Quantitative fluorescent intensity of different sections. (**f**) Representative fluorescence images of spheroids after 4 days incubation with the different NPs. Scale bars represent 150 μm. (Adapted with permission from Ref. [86])

tion and penetration of NPs in the tumor tissue after intravenous injection, validating the in vitro results. Antibodies can also be used as targeting moieties and tested in 3D cultures. Hortelão et al. [90] have modified mesoporous silica NPs with PEG and antibody anti-fibroblast growth factor receptor 3 (FGFR3), a protein overexpressed in bladder cancer, and

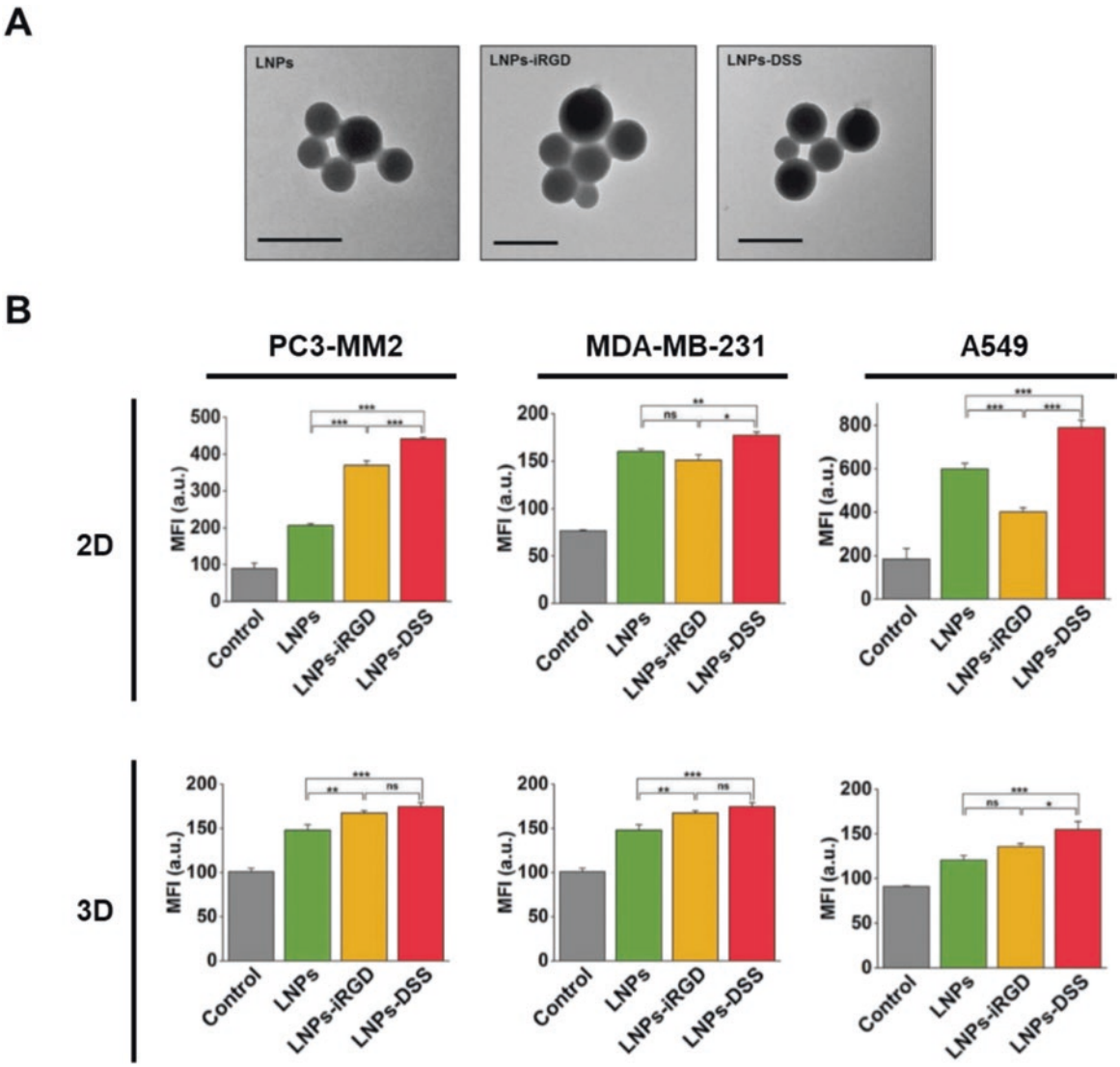

Fig. 6 (**a**) Transmission electron microscopy images of lignin NPs (LNPs) and lignin NPs modified with i-RGD (LNPs-iRGD) and with DSS (LNPs-DSS). Scale bars represent 200 nm. (**b**) Cellular uptake after incubation of unmodified and modified LNPs with either 2D monolayers or spheroids of PC3-MM2, MDA-MB-231, and A549 cells, for 3 h. Results represent mean ± s.d. ($n = 3$). Statistical significance was set at probabilities of $^{*}p < 0.05$, $^{**}p < 0.01$, and $^{***}p < 0.001$, and ns is nonsignificant. (Adapted with permission from Ref. [88])

analyzed their penetration and anticancer efficacy in bladder cancer MCTS. The modification with the antibody enhanced the internalization fourfold compared to the control and induced also antiproliferative effect due to the interaction between the antibody and antigen.

Other studies have also shown the increment of NP uptake by spheroids and deeper penetration when decorated with targeting moieties or coadministered with tumor-homing peptides [91–93]. However, it is necessary to take into consideration that several targeting strategies will only increase the uptake by the superficial layers, and an increment in the penetration will only be achieved if the uptake mechanisms are reversible and the NPs are released again from the cells [42, 94]. Moreover, there is also the possibility of coating the NPs' surface with ECM-degrading enzymes, such as collagenase, or loading the NPs with ECM-degrading drugs to increase their accumulation in the tumor tissue [95–97]. For example, Wang et al. [97] have shown that by functionalizing the surface of nanogels with collagenase, there was an increment on the penetration of the NPs into HepG2 MCTS due to ECM degradation, leading also to higher drug accumulation and enhanced growth inhibition. Furthermore, these results were also confirmed in in vivo assays, where the presence of collagenase leads to an enhanced tumor permeation and antitumor effect.

3.2 Cytocompatibility and Efficacy

MCTS, due to their morphological and biological differences when compared to 2D cultures, are an important tool to assess in vitro the biocompatibility and the anticancer efficacy of the developed NPs, as they might produce different results from 2D cultures [27]. For example, Shi et al. [65] reported much higher IC_{50} values for HCT116 and HCT-8 MCTS (16 and 17 μg/mL, respectively) compared to HCT116 and HCT-8 monolayers (1.4 and 1.1 μg/mL, respectively) after treating the cells with NPs loaded with the chemotherapeutic 5-fluorouracil. The same observation was made in several reports in the literature using various NPs and chemotherapeutics [98–101]. This shows an increased resistance of the cells when cultured in 3D compared to 2D which can be crucial when deciding dosages to test in vivo. Therefore, it must be taken into account when developing NPs for cancer therapy.

Also, since some NPs can promote toxic effect, for example, by promoting inflammation, it is important to develop in vitro models for risk assessment of NPs. In this regard, Leite et al. [102] have evaluated the neurotoxic effect of different types of NPs, gold NPs functionalized with sodium citrate or PEG and polylactic acid NPs, in two 3D neural models, of neurons (LUHMES) and of iPSC-derived brain spheroids. To do so, NPs were incubated with the spheroids, and their viability, morphology, secretion of cytokines, growth factors, and chemokines and gene expression were evaluated. In the monoculture model, NPs have demonstrated some degree of toxicity toward the neurons. However, when incubated with the more complex spheroid model, the NPs did not exert toxic effect probably due to the existent glial cells. Yet, gold NPs promoted some cell physiology alteration that might increase susceptibility to other harmful agents.

Other studies, as, for example, the one performed by Zhou et al. [103], demonstrate the applicability of the MCTS to predict the results in vivo. In this study, the authors developed Ru-Pt bimetallic metallacage encapsulated NPs (5-NPs) as photosensitizers for photodynamic therapy for cancer and tested them in 2D, 3D, and in vivo (Fig. 7). The developed 5-NPs were spherical and had size average of 260 nm. When tested in 2D monolayers of A549 lung cancer cells, these NPs were rapidly taken up, showed high cytocompatibility, and exerted increased toxicity when excited by light. Furthermore, 5-NPs have also shown high cytocompatibility in 3D A549 MCTS model and stimuli-dependent antiproliferative effect. In fact, after light irradiation, spheroids treated with NPs shrank to a volume of 80.4% after 1 day, while the control groups volume growth to ca. 180%. These results were confirmed in vivo, as there was a significant tumor

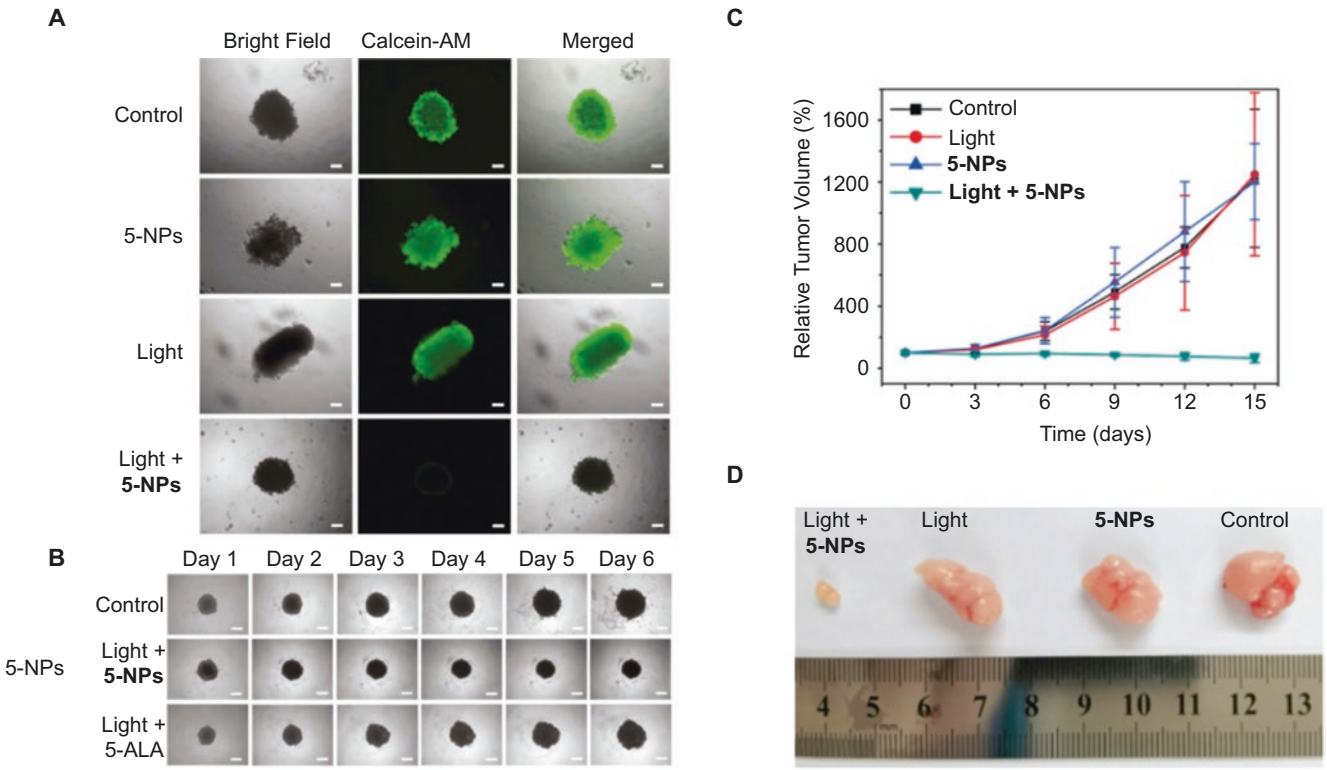

Fig. 7 (**a**) Spheroid viability. Representative confocal microscopy images of spheroids after treatment. (**b**) Representative bright-field images of spheroids after treatments. Scale bars represent 200 μm. (**c**) Mice tumor growth curve after different treatments. (**d**) Representative images of tumors in mice after different treatments. (Adapted with permission from Ref. [103])

reduction (to 65% of original volume) in A549 tumor-bearing animals treated with the 5-NPs intratumorally and irradiated by laser, when compared to the controls which had a 12-fold increase.

4 Conclusions and Future Perspectives

Currently, numerous NPs with different physicochemical characteristics and loaded with different anticancer molecules have been designed and tested for their efficacy in MCTS models and compared to their effect in vivo [42, 68]. Interestingly, the observed results in spheroids regarding NP penetration and accumulation, as well as their effect on tumor growth inhibition, are similar to the ones obtained in vivo [68]. Taking this into account, 3D cellular models, despite not being able to fully recreate every aspect of the tumor milieu, have shown to have a more physiological function than 2D cell cultures, with a consequent superior predictive effect than the 2D monoculture cell models [104, 105].

Despite MCTS being revolutionizing preclinical testing, there are still numerous challenges to be addressed before they can be applied as standard methods for NP testing. Firstly, the focus should be directed to the development of standardized protocols for spheroid formation and evaluation (e.g., metabolic activity, size, development of necrotic core). Next, the protocols for the different assays to assess NP interaction with cancer cells/MCTS should also be standardized (e.g., viability, cellular uptake, penetration, antiproliferative effect) in order to facilitate the comparison of results between different studies. Also, there is the need to perform systematic studies changing only one variable at a time, to allow the proper evaluation of its effect on 2D, 3D, and in vivo models. Finally, fully characterized MCTS models with higher complexity must be developed in order to further mimic the TME and create better predictive tools to ease the translation of NPs to the clinic.

Nevertheless, after surpassing the current challenges, MCTS models have the potential to become the gold-standard in vitro models to assess NPs, highly impacting the design of in vivo studies and accelerating the translation of the developed systems into the clinics.

Acknowledgments T. Bauleth-Ramos acknowledges financial support from Fundação para a Ciência e a Tecnologia (grant no. SFRH/BD/110859/2015). This work was financed by the project NORTE-01-0145-FEDER-000012 by Norte Portugal Regional Operational Programme (NORTE 2020), and COMPETE 2020 – Operacional Programme for Competitiveness and Internationalisation (POCI), under the PORTUGAL 2020 Partnership Agreement, through the (FEDER) Fundo Europeu de Desenvolvimento Regional and by Portuguese funds through (FCT) Fundação para a Ciência e a Tecnologia/Ministério da Ciência, Tecnologia e Ensino Superior in the framework of the project "Institute for Research and Innovation in Health Sciences" UID/BIM/04293/2019.

References

1. Bray, F., Ferlay, J., Soerjomataram, I., Siegel, R. L., Torre, L. A., & Jemal, A. (2018). Global cancer statistics 2018: GLOBOCAN estimates of incidence and mortality worldwide for 36 cancers in 185 countries. *CA: a Cancer Journal for Clinicians, 68*(6), 394–424.
2. Brannon-Peppas, L., & Blanchette, J. O. (2004). Nanoparticle and targeted systems for cancer therapy. *Advanced Drug Delivery Reviews, 56*(11), 1649–1659.
3. Chakraborty, S., & Rahman, T. (2012). The difficulties in cancer treatment. *Ecancermedicalscience, 6*, ed16.
4. Shi, J., Kantoff, P. W., Wooster, R., & Farokhzad, O. C. (2017). Cancer nanomedicine: Progress, challenges and opportunities. *Nature Reviews. Cancer, 17*(1), 20–37.
5. Peer, D., Karp, J. M., Hong, S., Farokhzad, O. C., Margalit, R., & Langer, R. (2007). Nanocarriers as an emerging platform for cancer therapy. *Nature Nanotechnology, 2*(12), 751–760.
6. van der Meel, R., Sulheim, E., Shi, Y., Kiessling, F., Mulder, W. J. M., & Lammers, T. (2019). Smart cancer nanomedicine. *Nature Nanotechnology, 14*(11), 1007–1017.
7. Figueiredo, P., Bauleth-Ramos, T., Hirvonen, J., Sarmento, B., & Santos, H. A. (2018). Chapter 1 – The emerging role of multifunctional theranostic materials in cancer nanomedicine. In J. Conde (Ed.), *Handbook of nanomaterials for cancer theranostics* (pp. 1–31). Elsevier: Amsterdam, The Netherlands.
8. Balasubramanian, V., Liu, Z., Hirvonen, J., & Santos, H. A. (2018). Bridging the knowledge of different worlds to understand the big picture of cancer nanomedicines. *Advanced Healthcare Materials, 7*(1), 1700432.
9. Hare, J. I., Lammers, T., Ashford, M. B., Puri, S., Storm, G., & Barry, S. T. (2017). Challenges and strategies in anti-cancer nanomedicine development: An industry perspective. *Advanced Drug Delivery Reviews, 108*, 25–38.
10. Shreffler, J. W., Pullan, J. E., Dailey, K. M., Mallik, S., & Brooks, A. E. (2019). Overcoming hurdles in nanoparticle clinical translation: The influence of experimental design and surface modification. *International Journal of Molecular Sciences, 20*(23), 6056.
11. Choi, S. Y., Lin, D., Gout, P. W., Collins, C. C., Xu, Y., & Wang, Y. (2014). Lessons from patient-derived xenografts for better in vitro modeling of human cancer. *Advanced Drug Delivery Reviews, 79–80*, 222–237.
12. Thoma, C. R., Zimmermann, M., Agarkova, I., Kelm, J. M., & Krek, W. (2014). 3D cell culture systems modeling tumor growth determinants in cancer target discovery. *Advanced Drug Delivery Reviews, 69–70*, 29–41.
13. Chatzinikolaidou, M. (2016). Cell spheroids: The new frontiers in in vitro models for cancer drug validation. *Drug Discovery Today, 21*(9), 1553–1560.
14. Niu, N., & Wang, L. (2015). In vitro human cell line models to predict clinical response to anticancer drugs. *Pharmacogenomics, 16*(3), 273–285.
15. Nunes, A. S., Barros, A. S., Costa, E. C., Moreira, A. F., & Correia, I. J. (2019). 3D tumor spheroids as in vitro models to mimic in vivo human solid tumors resistance to therapeutic drugs. *Biotechnology and Bioengineering, 116*(1), 206–226.
16. Ibarrola-Villava, M., Cervantes, A., & Bardelli, A. (2018). Preclinical models for precision oncology. *Biochimica Et Biophysica Acta. Reviews on Cancer, 1870*(2), 239–246.
17. Cifola, I., Bianchi, C., Mangano, E., Bombelli, S., Frascati, F., Fasoli, E., Ferrero, S., Di Stefano, V., Zipeto, M. A., Magni, F., Signorini, S., Battaglia, C., & Perego, R. A. (2011). Renal cell carcinoma primary cultures maintain genomic and phenotypic profile of parental tumor tissues. *BMC Cancer, 11*, 244.

18. Fabbrizi Maria, R., Duff, T., Oliver, J., & Wilde, C. (2014). Advanced in vitro systems for efficacy and toxicity testing in nanomedicine. *European Journal of Nanomedicine, 6*, 171.
19. Weiswald, L. B., Bellet, D., & Dangles-Marie, V. (2015). Spherical cancer models in tumor biology. *Neoplasia, 17*(1), 1–15.
20. Pampaloni, F., Reynaud, E. G., & Stelzer, E. H. K. (2007). The third dimension bridges the gap between cell culture and live tissue. *Nature Reviews Molecular Cell Biology, 8*(10), 839–845.
21. Xu, X., Farach-Carson, M. C., & Jia, X. (2014). Three-dimensional in vitro tumor models for cancer research and drug evaluation. *Biotechnology Advances, 32*(7), 1256–1268.
22. Klimkiewicz, K., Weglarczyk, K., Collet, G., Paprocka, M., Guichard, A., Sarna, M., Jozkowicz, A., Dulak, J., Sarna, T., Grillon, C., & Kieda, C. (2017). A 3D model of tumour angiogenic microenvironment to monitor hypoxia effects on cell interactions and cancer stem cell selection. *Cancer Letters, 396*, 10–20.
23. Baker, B. M., & Chen, C. S. (2012). Deconstructing the third dimension – how 3D culture microenvironments alter cellular cues. *Journal of Cell Science, 125*(13), 3015–3024.
24. Lamichhane, S. P., Arya, N., Kohler, E., Xiang, S., Christensen, J., & Shastri, V. P. (2016). Recapitulating epithelial tumor microenvironment in vitro using three dimensional tri-culture of human epithelial, endothelial, and mesenchymal cells. *BMC Cancer, 16*(1), 581.
25. Cavo, M., Fato, M., Peñuela, L., Beltrame, F., Raiteri, R., & Scaglione, S. (2016). Microenvironment complexity and matrix stiffness regulate breast cancer cell activity in a 3D in vitro model. *Scientific Reports, 6*, 35367.
26. Liu, T., Lin, B., & Qin, J. (2010). Carcinoma-associated fibroblasts promoted tumor spheroid invasion on a microfluidic 3D co-culture device. *Lab on a Chip, 10*(13), 1671–1677.
27. Shoval, H., Karsch-Bluman, A., Brill-Karniely, Y., Stern, T., Zamir, G., Hubert, A., & Benny, O. (2017). Tumor cells and their crosstalk with endothelial cells in 3D spheroids. *Scientific Reports, 7*(1), 10428.
28. Hirschhaeuser, F., Menne, H., Dittfeld, C., West, J., Mueller-Klieser, W., & Kunz-Schughart, L. A. (2010). Multicellular tumor spheroids: An underestimated tool is catching up again. *Journal of Biotechnology, 148*(1), 3–15.
29. Haycock, J. W. (2011). 3D Cell culture: A review of current approaches and techniques. In J. W. Haycock (Ed.), *3D cell culture: Methods and protocols* (pp. 1–15). Totowa: Humana Press.
30. Hutmacher, D. W., Horch, R. E., Loessner, D., Rizzi, S., Sieh, S., Reichert, J. C., Clements, J. A., Beier, J. P., Arkudas, A., Bleiziffer, O., & Kneser, U. (2009). Translating tissue engineering technology platforms into cancer research. *Journal of Cellular and Molecular Medicine, 13*(8a), 1417–1427.
31. Knight, E., & Przyborski, S. (2015). Advances in 3D cell culture technologies enabling tissue-like structures to be created in vitro. *Journal of Anatomy, 227*(6), 746–756.
32. Kunz-Schughart, L. A. (1999). Multicellular tumor spheroids: Intermediates between monolayer culture and in vivo tumor. *Cell Biology International, 23*(3), 157–161.
33. Huang, B.-W., & Gao, J.-Q. (2018). Application of 3D cultured multicellular spheroid tumor models in tumor-targeted drug delivery system research. *Journal of Controlled Release, 270*, 246–259.
34. Froehlich, K., Haeger, J.-D., Heger, J., Pastuschek, J., Photini, S. M., Yan, Y., Lupp, A., Pfarrer, C., Mrowka, R., Schleußner, E., Markert, U. R., & Schmidt, A. (2016). Generation of multicellular breast cancer tumor spheroids: Comparison of different protocols. *Journal of Mammary Gland Biology and Neoplasia, 21*(3), 89–98.
35. Achilli, T.-M., Meyer, J., & Morgan, J. R. (2012). Advances in the formation, use and understanding of multi-cellular spheroids. *Expert Opinion on Biological Therapy, 12*(10), 1347–1360.
36. Tung, Y.-C., Hsiao, A. Y., Allen, S. G., Torisawa, Y.-S., Ho, M., & Takayama, S. (2011). High-throughput 3D spheroid culture and drug testing using a 384 hanging drop array. *Analyst, 136*(3), 473–478.
37. Timmins, N. E., & Nielsen, L. K. (2007). Generation of multicellular tumor spheroids by the hanging-drop method. In H. Hauser & M. Fussenegger (Eds.), *Tissue engineering* (pp. 141–151). Totowa: Humana Press.
38. Sutherland, R. M., McCredie, J. A., & Inch, W. R. (1971). Growth of multicell spheroids in tissue culture as a model of nodular carcinomas. *JNCI: Journal of the National Cancer Institute, 46*(1), 113–120.
39. Tang, Y., Liu, J., & Chen, Y. (2016). Agarose multi-wells for tumour spheroid formation and anti-cancer drug test. *Microelectronic Engineering, 158*, 41–45.
40. Costa, E. C., de Melo-Diogo, D., Moreira, A. F., Carvalho, M. P., & Correia, I. J. (2018). Spheroids formation on non-adhesive surfaces by liquid overlay technique: Considerations and practical approaches. *Biotechnology Journal, 13*(1), 1700417.
41. Mehta, G., Hsiao, A. Y., Ingram, M., Luker, G. D., & Takayama, S. (2012). Opportunities and challenges for use of tumor spheroids as models to test drug delivery and efficacy. *Journal of Controlled Release, 164*(2), 192–204.
42. Lu, H., & Stenzel, M. H. (2018). Multicellular tumor spheroids (MCTS) as a 3D in vitro evaluation tool of nanoparticles. *Small, 14*(13), 1702858.
43. Gebhard, C., Gabriel, C., & Walter, I. (2016). Morphological and immunohistochemical characterization of canine osteosarcoma spheroid cell cultures. *Anatomia, Histologia, Embryologia, 45*(3), 219–230.
44. Kunz-Schughart, L. A., Freyer, J. P., Hofstaedter, F., & Ebner, R. (2004). The use of 3-D cultures for high-throughput screening: The multicellular spheroid model. *Journal of Biomolecular Screening, 9*(4), 273–285.
45. Lin, R.-Z., & Chang, H.-Y. (2008). Recent advances in three-dimensional multicellular spheroid culture for biomedical research. *Biotechnology Journal, 3*(9–10), 1172–1184.
46. Katt, M. E., Placone, A. L., Wong, A. D., Xu, Z. S., & Searson, P. C. (2016). In vitro tumor models: Advantages, disadvantages, variables, and selecting the right platform. *Frontiers in Bioengineering and Biotechnology, 4*, 12.
47. Rohwer, N., & Cramer, T. (2011). Hypoxia-mediated drug resistance: Novel insights on the functional interaction of HIFs and cell death pathways. *Drug Resistance Updates, 14*(3), 191–201.
48. Trédan, O., Galmarini, C. M., Patel, K., & Tannock, I. F. (2007). Drug resistance and the solid tumor microenvironment. *JNCI: Journal of the National Cancer Institute, 99*(19), 1441–1454.
49. Swietach, P., Hulikova, A., Patiar, S., Vaughan-Jones, R. D., & Harris, A. L. (2012). Importance of intracellular pH in determining the uptake and efficacy of the weakly basic chemotherapeutic drug, doxorubicin. *PloS One, 7*(4), e35949.
50. Majety, M., Pradel, L. P., Gies, M., & Ries, C. H. (2015). Fibroblasts influence survival and therapeutic response in a 3D co-culture model. *PLoS One, 10*(6), e0127948.
51. Lee, J. W., Shin, D. H., & Roh, J. L. (2018). Development of an in vitro cell-sheet cancer model for chemotherapeutic screening. *Theranostics, 8*(14), 3964–3973.
52. Correia, A. L., & Bissell, M. J. (2012). The tumor microenvironment is a dominant force in multidrug resistance. *Drug Resistance Updates, 15*(1), 39–49.
53. Sun, Y. (2016). Tumor microenvironment and cancer therapy resistance. *Cancer Letters, 380*(1), 205–215.
54. Pickup, M. W., Mouw, J. K., & Weaver, V. M. (2014). The extracellular matrix modulates the hallmarks of cancer. *EMBO Reports, 15*(12), 1243–1253.

55. Costa, E. C., Moreira, A. F., de Melo-Diogo, D., Gaspar, V. M., Carvalho, M. P., & Correia, I. J. (2016). 3D tumor spheroids: An overview on the tools and techniques used for their analysis. *Biotechnology Advances, 34*(8), 1427–1441.
56. Longati, P., Jia, X., Eimer, J., Wagman, A., Witt, M.-R., Rehnmark, S., Verbeke, C., Toftgård, R., Löhr, M., & Heuchel, R. L. (2013). 3D pancreatic carcinoma spheroids induce a matrix-rich, chemoresistant phenotype offering a better model for drug testing. *BMC Cancer, 13*(1), 95.
57. Nath, S., & Devi, G. R. (2016). Three-dimensional culture systems in cancer research: Focus on tumor spheroid model. *Pharmacology and Therapeutics, 163*, 94–108.
58. Ma, H.-L., Jiang, Q., Han, S., Wu, Y., Tomshine, J. C., Wang, D., Gan, Y., Zou, G., & Liang, X.-J. (2012). Multicellular tumor spheroids as an in vivo–like tumor model for three-dimensional imaging of chemotherapeutic and nano material cellular penetration. *Molecular Imaging, 11*(6), 7290.2012.00012.
59. Zanoni, M., Piccinini, F., Arienti, C., Zamagni, A., Santi, S., Polico, R., Bevilacqua, A., & Tesei, A. (2016). 3D tumor spheroid models for in vitro therapeutic screening: A systematic approach to enhance the biological relevance of data obtained. *Scientific Reports, 6*, 19103.
60. Fang, Y., & Eglen, R. M. (2017). Three-dimensional cell cultures in drug discovery and development. *Slas Discovery: Advancing Life Sciences R&D, 22*(5), 456–472.
61. Rodrigues, T., Kundu, B., Silva-Correia, J., Kundu, S. C., Oliveira, J. M., Reis, R. L., & Correlo, V. M. (2018). Emerging tumor spheroids technologies for 3D in vitro cancer modeling. *Pharmacology and Therapeutics, 184*, 201–211.
62. Hoarau-Véchot, J., Rafii, A., Touboul, C., & Pasquier, J. (2018). Halfway between 2D and animal models: Are 3D cultures the ideal tool to study cancer-microenvironment interactions? *International Journal of Molecular Sciences, 19*(1), 181.
63. Li, Y., Wang, J., Wientjes, M. G., & Au, J. L. S. (2012). Delivery of nanomedicines to extracellular and intracellular compartments of a solid tumor. *Advanced Drug Delivery Reviews, 64*(1), 29–39.
64. Ozcelikkale, A., Ghosh, S., & Han, B. (2013). Multifaceted transport characteristics of nanomedicine: Needs for characterization in dynamic environment. *Molecular Pharmaceutics, 10*(6), 2111–2126.
65. Shi, W. B., Le, V. M., Gu, C. H., Zheng, Y. H., Lang, M. D., Lu, Y. H., & Liu, J. W. (2014). Overcoming multidrug resistance in 2D and 3D culture models by controlled drug chitosan-graft poly(caprolactone)-based nanoparticles. *Journal of Pharmaceutical Sciences, 103*(4), 1064–1074.
66. Biondi, M., Guarnieri, D., Yu, H., Belli, V., & Netti, P. A. (2013). Sub-100 nm biodegradable nanoparticles: In vitro release features and toxicity testing in 2D and 3D cell cultures. *Nanotechnology, 24*(4), 045101.
67. Solomon, M. A., Lemera, J., & D'Souza, G. G. M. (2016). Development of an in vitro tumor spheroid culture model amenable to high-throughput testing of potential anticancer nanotherapeutics. *Journal of Liposome Research, 26*(3), 246–260.
68. Millard, M., Yakavets, I., Zorin, V., Kulmukhamedova, A., Marchal, S., & Bezdetnaya, L. (2017). Drug delivery to solid tumors: The predictive value of the multicellular tumor spheroid model for nanomedicine screening. *International Journal of Nanomedicine, 12*, 7993–8007.
69. Tchoryk, A., Taresco, V., Argent, R. H., Ashford, M., Gellert, P. R., Stolnik, S., Grabowska, A., & Garnett, M. C. (2019). Penetration and uptake of nanoparticles in 3D tumor spheroids. *Bioconjugate Chemistry, 30*(5), 1371–1384.
70. Durymanov, M., Kroll, C., Permyakova, A., & Reineke, J. (2019). Role of endocytosis in nanoparticle penetration of 3D pancreatic cancer spheroids. *Molecular Pharmaceutics, 16*(3), 1074–1082.
71. Huo, S., Ma, H., Huang, K., Liu, J., Wei, T., Jin, S., Zhang, J., He, S., & Liang, X. J. (2013). Superior penetration and retention behavior of 50 nm gold nanoparticles in tumors. *Cancer Research, 73*(1), 319–330.
72. Huang, K., Ma, H., Liu, J., Huo, S., Kumar, A., Wei, T., Zhang, X., Jin, S., Gan, Y., Wang, P. C., He, S., Zhang, X., & Liang, X. J. (2012). Size-dependent localization and penetration of ultrasmall gold nanoparticles in cancer cells, multicellular spheroids, and tumors in vivo. *ACS Nano, 6*(5), 4483–4493.
73. Albanese, A., Lam, A. K., Sykes, E. A., Rocheleau, J. V., & Chan, W. C. W. (2013). Tumour-on-a-chip provides an optical window into nanoparticle tissue transport. *Nature Communications, 4*(1), 2718.
74. Tang, L., Yang, X., Yin, Q., Cai, K., Wang, H., Chaudhury, I., Yao, C., Zhou, Q., Kwon, M., Hartman, J. A., Dobrucki, I. T., Dobrucki, L. W., Borst, L. B., Lezmi, S., Helferich, W. G., Ferguson, A. L., Fan, T. M., & Cheng, J. (2014). Investigating the optimal size of anticancer nanomedicine. *Proceedings of the National Academy of Sciences, 111*(43), 15344–15349.
75. Stylianopoulos, T., Poh, M.-Z., Insin, N., Bawendi, M. G., Fukumura, D., Munn, L. L., & Jain, R. K. (2010). Diffusion of particles in the extracellular matrix: The effect of repulsive electrostatic interactions. *Biophysical Journal, 99*(5), 1342–1349.
76. Suzuki, S., Itakura, S., Matsui, R., Nakayama, K., Nishi, T., Nishimoto, A., Hama, S., & Kogure, K. (2017). Tumor microenvironment-sensitive liposomes penetrate tumor tissue via attenuated interaction of the extracellular matrix and tumor cells and accompanying actin depolymerization. *Biomacromolecules, 18*(2), 535–543.
77. Jin, S., Ma, X., Ma, H., Zheng, K., Liu, J., Hou, S., Meng, J., Wang, P. C., Wu, X., & Liang, X. J. (2013). Surface chemistry-mediated penetration and gold nanorod thermotherapy in multicellular tumor spheroids. *Nanoscale, 5*(1), 143–146.
78. Lieleg, O., Baumgartel, R. M., & Bausch, A. R. (2009). Selective filtering of particles by the extracellular matrix: An electrostatic bandpass. *Biophysical Journal, 97*(6), 1569–1577.
79. Kostarelos, K., Emfietzoglou, D., Papakostas, A., Yang, W.-H., Ballangrud, Å., & Sgouros, G. (2004). Binding and interstitial penetration of liposomes within avascular tumor spheroids. *International Journal of Cancer, 112*(4), 713–721.
80. Ernsting, M. J., Murakami, M., Roy, A., & Li, S. D. (2013). Factors controlling the pharmacokinetics, biodistribution and intratumoral penetration of nanoparticles. *Journal of Controlled Release, 172*(3), 782–794.
81. Dias, D. R., Moreira, A. F., & Correia, I. J. (2016). The effect of the shape of gold core–mesoporous silica shell nanoparticles on the cellular behavior and tumor spheroid penetration. *Journal of Materials Chemistry B, 4*(47), 7630–7640.
82. Agarwal, R., Jurney, P., Raythatha, M., Singh, V., Sreenivasan, S. V., Shi, L., & Roy, K. (2015). Effect of shape, size, and aspect ratio on nanoparticle penetration and distribution inside solid tissues using 3D spheroid models. *Advanced Healthcare Materials, 4*(15), 2269–2280.
83. Wang, W., Gaus, K., Tilley, R. D., & Gooding, J. J. (2019). The impact of nanoparticle shape on cellular internalisation and transport: What do the different analysis methods tell us? *Materials Horizons, 6*(8), 1538–1547.
84. Lee, K. L., Hubbard, L. C., Hern, S., Yildiz, I., Gratzl, M., & Steinmetz, N. F. (2013). Shape matters: the diffusion rates of TMV rods and CPMV icosahedrons in a spheroid model of extracellular matrix are distinct. *Biomaterials Science, 1*(6), 581–588.
85. Chauhan, V. P., Popović, Z., Chen, O., Cui, J., Fukumura, D., Bawendi, M. G., & Jain, R. K. (2011). Fluorescent nanorods and nanospheres for real-time in vivo probing of nanoparticle shape-dependent tumor penetration. *Angewandte Chemie International Edition, 50*(48), 11417–11420.
86. Zhang, L., Wang, Y., Yang, D., Huang, W., Hao, P., Feng, S., Appelhans, D., Zhang, T., & Zan, X. (2019). Shape effect of

nanoparticles on tumor penetration in monolayers versus spheroids. *Molecular Pharmaceutics, 16*(7), 2902–2911.
87. You, Y., Hu, H., He, L., & Chen, T. (2015). Differential effects of polymer-surface decoration on drug delivery, cellular retention, and action mechanisms of functionalized mesoporous silica nanoparticles. *Chemistry – An Asian Journal, 10*(12), 2744–2754.
88. Figueiredo, P., Sipponen, M. H., Lintinen, K., Correia, A., Kiriazis, A., Yli-Kauhaluoma, J., Österberg, M., George, A., Hirvonen, J., Kostiainen, M. A., & Santos, H. A. (2019). Preparation and characterization of dentin phosphophoryn-derived peptide-functionalized lignin nanoparticles for enhanced cellular uptake. *Small, 15*(24), 1901427.
89. Wang, Y., Yin, S., Mei, L., Yang, Y., Xu, S., He, X., Wang, M., Li, M., Zhang, Z., & He, Q. (2020). A dual receptors-targeting and size-switchable "cluster bomb" co-loading chemotherapeutic and transient receptor potential ankyrin 1 (TRPA-1) inhibitor for treatment of triple negative breast cancer. *Journal of Controlled Release, 321*, 71–83.
90. Hortelão, A. C., Carrascosa, R., Murillo-Cremaes, N., Patiño, T., & Sánchez, S. (2019). Targeting 3D bladder cancer spheroids with urease-powered nanomotors. *ACS Nano, 13*(1), 429–439.
91. Fan, R., Chuan, D., Hou, H., Chen, H., Han, B., Zhang, X., Zhou, L., Tong, A., Xu, J., & Guo, G. (2019). Development of a hybrid nanocarrier-recognizing tumor vasculature and penetrating the BBB for glioblastoma multi-targeting therapy. *Nanoscale, 11*(23), 11285–11304.
92. Hu, C., Yang, X., Liu, R., Ruan, S., Zhou, Y., Xiao, W., Yu, W., Yang, C., & Gao, H. (2018). Coadministration of iRGD with multistage responsive nanoparticles enhanced tumor targeting and penetration abilities for breast cancer therapy. *ACS Applied Materials & Interfaces, 10*(26), 22571–22579.
93. Marino, A., Camponovo, A., Degl'Innocenti, A., Bartolucci, M., Tapeinos, C., Martinelli, C., De Pasquale, D., Santoro, F., Mollo, V., Arai, S., Suzuki, M., Harada, Y., Petretto, A., & Ciofani, G. (2019). Multifunctional temozolomide-loaded lipid superparamagnetic nanovectors: Dual targeting and disintegration of glioblastoma spheroids by synergic chemotherapy and hyperthermia treatment. *Nanoscale, 11*(44), 21227–21248.
94. Chariou, P. L., Lee, K. L., Pokorski, J. K., Saidel, G. M., & Steinmetz, N. F. (2016). Diffusion and uptake of tobacco mosaic virus as therapeutic carrier in tumor tissue: Effect of nanoparticle aspect ratio. *The Journal of Physical Chemistry B, 120*(26), 6120–6129.
95. Goodman, T. T., Olive, P. L., & Pun, S. H. (2007). Increased nanoparticle penetration in collagenase-treated multicellular spheroids. *International Journal of Nanomedicine, 2*(2), 265–274.
96. Zhang, Y., Liu, Y., Gao, X., Li, X., Niu, X., Yuan, Z., & Wang, W. (2019). Near-infrared-light induced nanoparticles with enhanced tumor tissue penetration and intelligent drug release. *Acta Biomaterialia, 90*, 314–323.
97. Wang, X., Luo, J., He, L., Cheng, X., Yan, G., Wang, J., & Tang, R. (2018). Hybrid pH-sensitive nanogels surface-functionalized with collagenase for enhanced tumor penetration. *Journal of Colloid and Interface Science, 525*, 269–281.
98. Miranda, M. A., Marcato, P. D., Carvalho, I. P. S., Silva, L. B., Ribeiro, D. L., Amaral, R., Swiech, K., Bastos, J. K., Paschoal, J. A. R., dos Reis, R. B., & Bentley, M. V. L. B. (2019). Assessing the cytotoxic potential of glycoalkaloidic extract in nanoparticles against bladder cancer cells. *Journal of Pharmacy and Pharmacology, 71*(10), 1520–1531.
99. Ishiguro, S., Cai, S., Uppalapati, D., Turner, K., Zhang, T., Forrest, W. C., Forrest, M. L., & Tamura, M. (2016). Intratracheal administration of hyaluronan-cisplatin conjugate nanoparticles significantly attenuates lung cancer growth in mice. *Pharmaceutical Research, 33*(10), 2517–2529.
100. Godugu, C., Patel, A. R., Desai, U., Andey, T., Sams, A., & Singh, M. (2013). AlgiMatrix™ based 3D cell culture system as an in-vitro tumor model for anticancer studies. *PLoS One, 8*(1), e53708.
101. Affram, K. O., Smith, T., Ofori, E., Krishnan, S., Underwood, P., Trevino, J. G., & Agyare, E. (2020). Cytotoxic effects of gemcitabine-loaded solid lipid nanoparticles in pancreatic cancer cells. *Journal of Drug Delivery Science and Technology, 55*, 101374.
102. Leite, P. E. C., Pereira, M. R., Harris, G., Pamies, D., dos Santos, L. M. G., Granjeiro, J. M., Hogberg, H. T., Hartung, T., & Smirnova, L. (2019). Suitability of 3D human brain spheroid models to distinguish toxic effects of gold and poly-lactic acid nanoparticles to assess biocompatibility for brain drug delivery. *Particle and Fibre Toxicology, 16*(1), 22.
103. Zhou, Z., Liu, J., Huang, J., Rees, T. W., Wang, Y., Wang, H., Li, X., Chao, H., & Stang, P. J. (2019). A self-assembled Ru–Pt metallacage as a lysosome-targeting photosensitizer for 2-photon photodynamic therapy. *Proceedings of the National Academy of Sciences, 116*(41), 20296–20302.
104. Ramgolam, K., Lauriol, J., Lalou, C., Lauden, L., Michel, L., de la Grange, P., Khatib, A.-M., Aoudjit, F., Charron, D., Alcaide-Loridan, C., & Al-Daccak, R. (2011). Melanoma spheroids grown under neural crest cell conditions are highly plastic migratory/invasive tumor cells endowed with immunomodulator function. *PLoS One, 6*(4), e18784.
105. Horman, S. R., Hogan, C., Reyes, K. D., Lo, F., & Antczak, C. (2015). Challenges and opportunities toward enabling phenotypic screening of complex and 3D cell models. *Future Medicinal Chemistry, 7*(4), 513–525.
106. Priwitaningrum, D. L., Blondé, J.-B. G., Sridhar, A., van Baarlen, J., Hennink, W. E., Storm, G., Le Gac, S., & Prakash, J. (2016). Tumor stroma-containing 3D spheroid arrays: A tool to study nanoparticle penetration. *Journal of Controlled Release, 244*, 257–268.
107. Wang, H.-X., Zuo, Z.-Q., Du, J.-Z., Wang, Y.-C., Sun, R., Cao, Z.-T., Ye, X.-D., Wang, J.-L., Leong, K. W., & Wang, J. (2016). Surface charge critically affects tumor penetration and therapeutic efficacy of cancer nanomedicines. *Nano Today, 11*(2), 133–144.